MINISTRY OF EDUCATION AND TRAINING

VIETNAM ACADEMY OF SCIENCE AND TECHNOLOGY

GRADUATE UNIVERSITY OF SCIENCE AND TECHNOLOGY

……..….*……**

NGUYEN QUANG BAC

Synthesis of CeO_2-based nanocomposites and application for UV protection of the polyurethane coating

SUMMARY OF DISSERTATION ON INORGANIC CHEMISTRY

Code: 9 44 01 13

Hanoi – 2024

The dissertation is completed at: Graduate University of Science and Technology, Vietnam Academy Science and Technology

Supervisors:
Supervisor 1: Assoc. Prof. Dr Dao Ngoc Nhiem
Supervisor 2: Prof. Dr. Tran Dai Lam

Referee 1: Assoc. Prof. Dr. Nguyen Thi Thanh Chi
Referee 1: Assoc. Prof. Dr. Nguyen Minh Ngoc
Referee 3: Assoc. Prof. Dr. Le Thi Trinh

The dissertation will be examined by Examination Board of Graduate University of Science and Technology, Vietnam Academy of Science and Technology at 9 am 30th of May 2024.

The dissertation can be found at:
1. Graduate University of Science and Technology Library
2. National Library of Vietnam

Introduction

1. Motivation behind selecting the thesis topic

Polymers such as polyurethane (PU) and polyester have been widely utilized in many applications including transportation, interior design, automotive, and textile industry [1,2]. Recently, the PU market has experienced significant growth [3], indicating the scientific community's interest in developing this type of material. However, despite its relatively high durability, the PU coating still degrades when exposed to prolonged UV irradiation, high temperatures, humidity, oxygen, and some pollutants [4]. This degradation reduces the lifespan of the coating, necessitating the development of new methods to enhance its effectiveness.

The additives are dispersed into the PU coating at a very low concentration to avoid affecting the inherent properties of PU. These additives are added with the purpose of minimizing the photodegradation effects caused by UV light. The first method is based on the conjugated π system present in organic compounds. This conjugated system has the ability to absorb UV photons, such as ureido-pyrimidone and coumarine [5]. However, a limitation of these organic additives is that they themelves are susceptible to degradation when exposed to UV radiation over a prolonged period [6]. Furthermore, another limitation involves their low molecular weight, which leads to a tendency for self-escape from the substrate material. This loss leads to a modification in the structure of the PU coating layer, as well as a rapid decrease in its UV resistance.

The second method utilizes inorganic additives such as nanoparticles like CeO_2, ZnO, TiO_2, Fe_2O_3, or graphene. These inorganic materials have advantages such as non-volatility, immobility, lightness, thermal stability, and chemical stability [4]. Among these materials, nano CeO_2 is particularly of interest due to its unique properties such as high stability, high durability, and non-toxicity. This material has a bandgap of around 3.25 eV, which suitable for UV absorber [7]. Furthermore, the rapid electronic recombination enhances the UV protection efficiency of CeO_2 particles [8]. Dao et al. (2011) demonstrated that the UV absorption properties of epoxy films were significantly enhanced using a very small amount of CeO_2 nanoparticles [9]. However, nanomaterials often have the drawback of being difficult to disperse evenly in organic films due to their strong tendency to self-aggregate. Therefore, efforts have been made to achieve a stable and uniform distribution of CeO_2 by combining it with other oxides such as TiO_2 and SiO_2. In addition, the addition of SiO_2 has the ability to trap electrons excited by UV photons and convert them into thermal energy, which also means that UV degradation is prevented [10].

Due to the reasons mentioned above, I am doing a thesis on " **Synthesis of CeO_2-based nanocomposites and application for UV protection of the polyurethane coating**". This research is expected to provide highly applicable results.

2. Objectives

This dissertation was conducted with the following specific objectives:

- The synthesis of CeO_2-based nanocomposite materials using the gel combustion method results in particles with a size less than 50 nm and a stable structure.
- The synthesized nanocomposite materials are dispersed into the polyurethane coating by an in-situ polymerization method.
- Assessing the mechanical properties and UV resistance of the PU coating before and after dispersion of various nanocomposite material systems.

3. Specific content

- Information about polyurethane (PU) and applications of nanomaterials in enhancing coating properties.
- Synthesis and morphological investigation of nanomaterials using the gel combustion method with polyvinyl alcohol as a precursor.
- Dispersion and influence of CeO_2-based nanocomposite materials on the thermal stability and mechanical properties of PU coating.
- Investigation of the impact of CeO_2-based nanocomposite materials on long-term UV resistance under UV light exposure.

Research subject:

The topic focuses on the synthesis of nanomaterials (including CeO_2, CeO_2-SiO_2, CeO_2-Fe_2O_3@SiO_2) using the PVA gel combustion method. The study investigates the characteristic properties of the materials obtained and the properties of the PU coating before and after being dispersed with various nano-materials.

Methodology:

Utilize modern physical methods to characterize materials, such as PVA method, TG-DTA, XRD, SEM, TEM, SEM-EDX, UV-Vis, FT-IR. Particularly, the durability of the PU coating including CeO_2-based nanocomposite material before and after exposure to UV light is assessed according to HES D 6501 standard.

4. The scientific and practical significance

CeO_2-based nanocomposite materials with a size of less than 50 nm were synthesized by the gel combustion of PVA.

Dispersion of prepared nanocomposites in PU matrix to provide good UV protection and high weather resistance, making it suitable for use in coatings.

Contributes to the effective use of domestic rare earth minerals in general and CeO_2 as an additive for the industrial coating industry.

5. The contributions of the dissertation

- CeO_2-based nanocomposite materials, including CeO_2, CeO_2-SiO_2, and CeO_2-Fe_2O_3@SiO_2, were successfully produced utilizing the PVA gel combustion process. The nanomaterials obtained are highly stable and exhibit a size less than 50 nm, giving them well-suited for dispersion into a polyurethane (PU) matrix by an in-situ polymerization technique.

- Various physical properties of the PU coating that contains these CeO_2-based nanocomposite materials were assessed including durability, gloss, and color deviation using the HES D 6501 standard. Our findings indicate that only

a small amount (less than 1.0%) of these nanocomposite materials dispersed into the PU coating, the coating exhibits superior UV resistance and high weather resistance compared to standard PU.

MAIN CONTENT OF DESSERTATION

Chapter 1: INTRODUCTION

1.1. An overview of the application of nano materials for polyurethane coatings.

Although nano materials in PU coatings provide several benefits, their application nevertheless poses some obstacles. Nanoparticles have a tendency to clump together because of their significant ratio of surface area to particle size, their high surface tension, and their inability to mix well with water or most polymer substrates. It is crucial to carefully consider the dispersion and stability of nano particles in the PU matrix, as well as their compatibility with other coating components [24]. Various strategies have been explored to produce efficient dispersion of nanoparticles in PU coating. The process includes the utilization of surfactants, intense mixing techniques (such as ultrasonic and high shear mixing), and altering the surface properties of nano particles to improve their compatibility with PU substrates [20,26,27]. Through the process of optimizing dispersion, researchers can guarantee the even spread of nano particles, therefore maximizing their advantageous impact on the qualities of the coating. The durability of nanoparticles in the PU coating is another crucial issue to take into account. Over time, tiny particles can aggregate or silt, leading to the deterioration of their intended properties. In order to tackle this problem, scientists have investigated the application of surface modification methods to improve the durability of nanoparticles in a PU matrix [27]. Surface modification can be achieved by adding functional groups or polymer chains, which helps to avoid aggregation and enhance the stability of the coating layer [28]. Moreover, the choice of suitable nano particles and their concentration can also have a significant impact on preserving compatibility and achieving optimal performance.

1.2. Structure and properties of polyurethane

1.3. Methods for synthesizing PU

1.3.1. One-step synthesis method of PU

1.3.2. Two-step synthesis method of PU

1.4. Enhancing the UV resistance of the PU coating by the use of additives.

1.4.1. General principles for enhancing UV resistance

1.4.2. Enhancing UV resistance with inorganic nanotechnology

1.5. Nanomaterials based on CeO_2 used in polyurethane coating

1.5.1. General introduction to CeO_2 nano materials.

1.5.2. Applications of CeO_2 nano materials.

1.5.2.1. Research status outside of Vietnam.

a) Enhance the durability of the coating by using CeO_2-based nanomaterials.

b) Enhancing UV resistance by using CeO_2-based nanomaterials

CeO_2 has significant light absorption at around 370 nm in the ultraviolet (UV) region, like that of nano-TiO_2. All of these oxides are semiconducting materials with a band gap width of around 3.0-3.25 eV and demonstrate mechanisms of UV absorption. When a photon with energy greater than the bandgap energy is absorbed, it will create an electron-hole pair (h+/e-). In the case of TiO_2, the vacancies and electrons go towards the surface of the nano particles instead of mixing with each other inside the particles. Hydrogen or electrons present on the surface can undergo reactions with oxygen, water, or hydroxyl to generate free radicals. Free radicals are agents that undergo oxidation and can lead to the destruction of organic molecules, especially polymers, hence worsening the photodegradation of the coating layer. In contrast, CeO_2 has the ability to absorb UV light without experiencing any erosion of the coating layer by photocatalysis [48]. This is accomplished by the fast recombination of hydrogen ions (H+) and electrons (e-) within the CeO_2 crystal, preventing their migration to the surface as a result of crystal defects and redox processes. Consequently, there is no further production of free radicals. The process is shown using response equations (1)-(3), whereas equations (4)-(6) depict the interior dynamics of the crystal when it is triggered by a photon [79].

1.5.2.2. Research status in Vietnam

National researchers are familiar with rare earth materials in general, and especially CeO_2 compounds. The Vietnam National University and the Vietnam Academy of Science and Technology have shown a great interest in studying this particular material for a considerable period of time. Nanomaterials based on CeO_2 are utilized for many applications, including serving as catalytic materials for the treatment of hazardous organic compounds, water contaminants, and exhaust emissions. Dr. Pham Tien Duc's research group utilized CeO_2@SiO_2 material to treat antibiotics, namely methyl blue [80]. The research team, headed by Dr. Dao Ngoc Nhiem, has specifically done investigations on synthesizing a range of materials, including nano CeO_2, La_2O_3-CeO_2, CeO_2-Fe_2O_3, CeO_2-Al_2O_3, CuO-CeO_2, and their applications in diverse domains such as pollution treatment [81-83], gas treatment, and gas oxidation [84,85].

Research on the use of CeO_2 in polymer coatings remains significantly restricted. There has been a notable surge in interest in utilizing CeO_2-based nano materials as additives for novel polymer coatings in the past several years [86,87]. Dr. Dao Ngoc Nhiem's research group has used materials like CeO_2-TiO_2 and CeO_2 in epoxy and PU coatings [9,18]. Professor Dr. Tran Dai Lam's research group has successfully employed SiO_2@Ce materials to efficiently inhibit corrosion in steel [87]. The findings demonstrate that the incorporation of a small quantity of nano materials into coatings greatly improves the protective efficacy of the coatings against corrosion agents or UV radiation.

Prior research has repeatedly shown that the use of nano CeO_2 has several drawbacks, including a pronounced propensity for particle agglomeration due to their extremely tiny size. Consequently, the capacity to reuse catalysts in

applications would drop dramatically, and there will be difficulties in dispersing them into polymer matrices for additive applications. Moreover, the strong propensity of CeO_2 to initiate photocatalysis in the presence of extended outdoor humidity is the fundamental reason for polymer degradation (equations (7)-(8)). The unoccupied h+ sites will undergo a reaction with moisture, resulting in the production of free radicals. In addition, CeO_2 is quite costly in comparison to some other materials.

An area of study with great promise involves the utilization of SiO_2 substrate materials, which provide desirable characteristics such as high chemical stability and cheap cost. In addition, the use of SiO_2 has notable benefits, including the improvement of mechanical strength [55,88] and the provision of hydrophobic properties to the surface coating [89]. In addition, the SiO2 structure possesses cavities that can capture produced electrons, hence diminishing the effects of UV radiation [10,90]. Nevertheless, a drawback of nanoparticles in general is their inadequate dispersion in polymer matrix and their steady reduction in size. Prior research endeavors have made efforts to alter the surface characteristics of SiO_2 with the aim of improving its ability to disperse. Multiple investigations have suggested that the incorporation of CeO_2 and SiO_2 improves the ability of the polymer matrix to disperse. The Ye group and their colleagues have applied CeO2 onto the surface of SiO_2 nanoparticles to improve dispersion and hence boost the UV resistance of the fluorinated polyacrylate coating layer [91]. Xuwen and his colleagues, together with Wang and his colleagues, produced CeO_2@SiO_2 nanoparticles that have a core-shell structure in order to improve the dispersion and resistance to wear in polymers [92,93]. Nevertheless, the material formed can possess dimensions of up to 360 nm [91], which might potentially result in notable alterations in the color of the coating.

In addition, Fe_2O_3 is a cost-effective, long-lasting, and eco-friendly substance that has been used to improve the heat resistance of several polymers [94,95]. Furthermore, the incorporation of Fe_2O_3 also imparts advantageous characteristics such as resistance to corrosion and strong adherence for the polymer coating [96]. Palimi et al. found that applying a silane treatment to nano-Fe_2O_3 has led to a notable enhancement in the mechanical characteristics of the PU coating. The most notable enhancement is observed when nano-Fe_2O_3 is altered with 3g of silane [96]. In addition, the transformation from Fe_2O_3 to Fe_3O_4 increases the number of oxygen vacancies, which efficiently captures electrons during the photocatalytic reaction of CeO_2 [97]. As a result, the UV resistance of the PU coating that contains CeO_2 is indirectly improved.

1.5.3. Synthesis of nano materials based on CeO_2

1.6. The method of dispersing nanocomposite materials in a polyurethane matrix.

1.6.1. Thermal processing

1.6.2. Mixing of solutions

1.6.3. In-situ synthesis

Chapter 2. METHODOLOGY

2.1. Materials

2.1.1. Chemicals

All the chemicals used for material synthesis in this thesis include polyvinyl alcohol (PVA, M=145000 g.mol-1, 99%, Merck), cerium(III) nitrate hexahydrate ($Ce(NO_3)_3.6H_2O$, 99%, Merck), tetraethyl orthosilicate (TEOS, $Si(OC_2H_5)_4$, 99%, Merck), iron(III) nitrate nonahydrate ($Fe(NO_3)_3 \cdot 9H_2O$, 99%, Merck), 25% ammonium hydroxide solution (NH_4OH, Merck), and acetic acid (CH_3COOH, 99%, Merck). The chemicals used to prepare the polyurethane film include diisocyanate (Desmodur®Z 4470 MPA/X), two acrylic polyols (Acrydic AC-3252 and Olester AO-529), and other organic solvents. They are manufactured to industrial standards using commercial sources such as BASF Vietnam, TOP Solvent Vietnam, Evonik Singapore, Covestro Hong Kong, and Hunan Chemical China. All chemicals are used without the need for further refinement.

2.1.2. Equipment

The equipment used in this dissertation includes: Nabertherm 30-3000 °C furnace (Germany), Memmert UN110 drying cabinet (Germany), ATV-FH1200 vacuum cabinet (Vietnam), Ohaus PRseries electronic balance with a precision of 10^{-4} (USA), IKA Ceramag Midi hotplate stirrer (Netherlands), mercury thermometer, and Hidrolen 1300 rpm stirrer (Japan). The SevenCompact™ pH/Ion Meters (S220, METTLER TOLEDO®, USA) are pH measuring devices. The equipment includes: a heat-resistant beaker with a capacity of 50-500 mL, a graduated cylinder with a range of 10-1000 mL, and a pipette.

The synthesis of nano materials is conducted in the Inorganic Materials Laboratory, Materials Science Institute. Meanwhile, experiments on dispersing nano materials into the PU matrix and determining the characteristic properties of the coating such as mechanical properties, glossiness, and color deviation were conducted at the EASON URAI Vietnam factory. In addition, an experiment on weathering acceleration in the QUV weathering chamber was conducted at this factory to verify the durability of the PU coating.

2.2. Synthesis of nanomaterials

2.2.1. Synthesis of nano CeO_2, nano Fe_2O_3, nano SiO_2

2.2.2. Synthesis of nanocomposites CeO_2-SiO_2

2.2.3. Synthesis of nanocomposites CeO_2-Fe_2O_3@SiO_2

2.2.3.1. Synthesis of nano SiO_2

2.2.3.2 Synthesis of nano CeO_2-Fe_2O_3@SiO_2

0.434 g of $Ce(NO_3)_3.6H_2O$ and 0.350 g of $Fe(NO_3)_3.9H_2O$ (in a 1:1 molar ratio) are added to 55.8 mL of a 5.0% PVA solution. The pH of the solution is adjusted to 4.0 by adding a 1M solution of CH_3COOH and a 25% solution of NH_4OH. Afterwards, an additional 2.99 g of synthesized nano SiO_2 particles were added. This mixture is stirred at 80 °C for 4 hours until it forms a homogeneous gel. The gel is dried at 105 °C for 8 hours before being heated

at 550 °C, 650 °C, 750 °C, and 850 °C for 2 hours to investigate the phase formation of CeO_2-Fe_2O_3@SiO_2 (**CFS**-NC) material, which serves as a basis for selecting the optimal synthesis conditions for **CFS**-NC material.

2.2.4. Dispersion of prepared materials into PU coating

Weigh an equivalent amount of nano CeO_2, nano SiO_2, or nano Fe_2O_3 particles that have been synthesized in the previous section. Afterwards, disperse in acrylic polyol, solvent, and grinding aid additives. After mechanically stirring for 15 min, the mixture is crushed for eight cycles (30 mins/cycle). When the mixture is introduced into the centrifuge, it is filtered through a 37 μm filter and adjusted with a solvent to 100 g. The base paint is mixed with isocyanate curing agent and solvent for an additional 30 minutes, resulting in a viscosity of the mixture of 12.5 $m^2.s^{-1}$. The mixture is sprayed with an IWATA W71 paint gun onto cellophane to test its mechanical properties and UV resistance.

2.2.4.1. Dispersion of CeO_2 nanomaterials into polyurethane coating

2.2.4.2. Dispersion of nanocomposite CeO_2-SiO_2, CeO_2 -Fe_2O_3@SiO_2 into polyurethane coating

2.3. Materials characterization

2.3.1. Thermalgravimetric analysis (TGA)

The dried gel obtained from **section 2.2** was analyzed using TGA-DTA technique using the Labsys Evo instrument (France) at the Institute of Materials Science, Vietnam Academy of Science and Technology. Meanwhile, the thermal durability was investigated using the TGA-DSC method on the same device. The experimental conditions typically range from room temperature to 800 °C, in ambient air, with a heating rate of 10°.min^{-1}.

2.3.2. X-ray diffraction (XRD)

The prepared materials were characterized for their structural properties using X-ray diffraction (XRD) method on a Bruker D8 Advance instrument with Cu (Kα) radiation source at the Institute of Chemistry, Vietnam Academy of Science and Technology. The scanning angle typically ranges from 10° to 80°.

2.3.3. Electron microscopy method (SEM, TEM)

The nano materials synthesized in this dissertation were characterized for their morphological features using SEM and TEM techniques using the Hitachi S-4800 microscope (Japan). Meanwhile, SEM-EDS analysis is conducted using the 2100 HSX JEOL instrument from Japan. Both devices are operated by the Institute of Materials Science, Vietnam Academy of Science and Technology.

2.3.4. Ultraviolet-Visible spectroscopy (UV-Vis)

The light absorption capacity of nano materials is evaluated using a UV/Vis-DR spectrophotometer, namely the Cary UV-5000 spectrophotometer at Hanoi National University of Education.

2.3.5. Fourier-transform infrared spectroscopy (FT-IR)

The products including nanomaterials and PU coating were characterized using the Bruker Equinox 55 spectrometer (Germany) at the Institute of

Tropical Technology, Vietnam Academy of Science and Technology. The applied conditions for the materials in this thesis are within the wavelength range of 4000 cm^{-1} - 650 cm^{-1} and a scanning frequency of 64 times. In addition, the results were also compared with the measurement method using the ATR probe with the Cary 600 system (Agilent, USA) at the Institute of Geography, Vietnam Academy of Science and Technology.

2.3.6. Methods of analyzing coating properties

The testing method for paint according to HES D 6501 standard and all related measurements for the PU coating layer are conducted at EASON URAI Vietnam factory. The paint inspection will be conducted on the entire panel, which has been manufactured to be compatible with the paint's characteristics. The trial sample will be carried out on the entire panel, or a prototype using the same materials on the entire panel and paint under similar conditions.

2.3.6.1. Dry film thickness: Byko-test 4500

2.3.6.2. Gloss of the film using the BYK gloss meter with 3 angles: 20/60/85°

2.3.6.3. Measure color deviation: Cr-400

2.3.6.4. Measure water contact angle

2.3.6.5. Mechanical durability of the coating layer

2.3.7. Experiment testing weather acceleration in the QUV chamber

Chapter 3. RESULTS AND DISCUSSION

3.1. Characterization of nano CeO_2, nano Fe_2O_3, and nano SiO_2

3.1.1. Characteristics of the structure and morphology of nano CeO_2

3.1.1.1. Thermalgravimetric analysis of the gel (Ce^{3+}+PVA)

The TG-DTA diagram in **Figure 3.1** illustrates two mass reduction effects throughout the temperature increase from room temperature to 650 °C.The first mass reduction effect is around 55.9% within the temperature range of 50 to 200 degrees. The decrease corresponds to a heat dissipation effect at 185°C along the path. The deficit in mass is caused by the evaporation of remaining water in the gel and the decomposition of a portion of the organic components.The PVA fabric exhibits a secondary mass reduction effect within the temperature range of 400 to 500 °C, corresponding to a peak in thermal intensity emission.The DTA pathway. The cause is the oxidation reaction that decomposes the organic components in the gel sample and the combustion of the remaining precursors in the sample or intermediates in the formation of CeO_2 such as -NO_3. The mass loss was recorded ~34.45%. At a calcination temperature > 500 °C, the mass of the sample remained almost unchanged, indicating that the product CeO_2 could be formed and the precursors were burned out.

3.1.1.2. TEM, SEM images of nano CeO_2

In this dissertation, all nano materials are synthesized using the gel combustion method from the precursor PVA due to its exceptional characteristics. Specifically, the synthesis mechanism of materials using PVA gel is presented as follows: The presence of PVA in the aqueous solution provides hydroxyl groups (-OH) that can act as ligands for metal cations and

long hydrocarbon chains (**Figure 3.3**). Therefore, metal cations are surrounded by carbon chains in the form of M-$(OH)_n$ complexes. PVA encapsulates and severs metal ions, preventing their aggregation. The result is that metal ions do not grow in size and do not precipitate, leading to the formation of a cage-like structure inside the high molecular structure of PVA [118]. PVA subsequently functions as an organic fuel during the combustion process. The obtained nanoparticles are spherical in shape, very pure, and uniform [119].

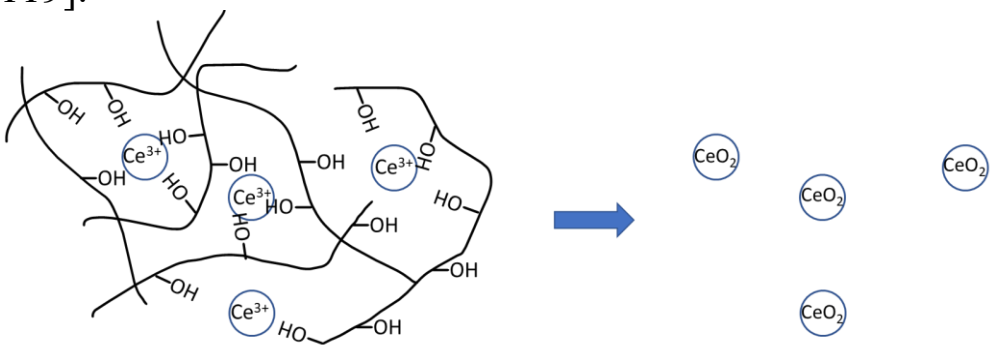

Figure 3.1. The mechanism of nanostructure formation in the combustion of PVA gel.

3.1.1.3. XRD pattern of nano CeO_2 with calcination temperature of 550 °C

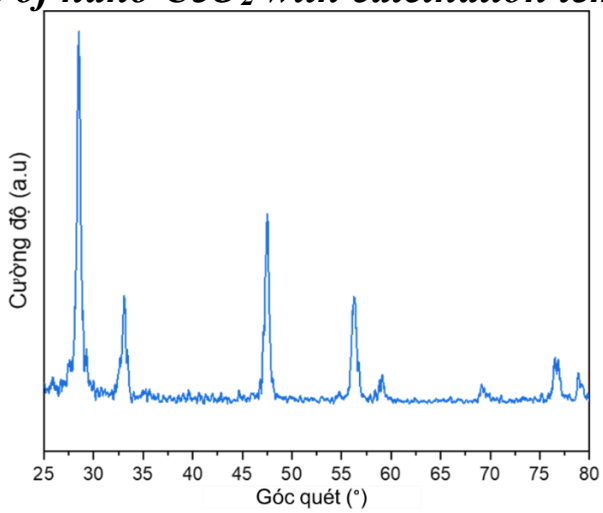

Figure 3.2. The XRD pattern of CeO_2 nanoparticles synthesized at a calcination temperature of 550 °C.

Evidently, the material exhibits excellent crystallinity. The intensity of the distinctive peaks is high, sharp, and the bases of the distinctive peaks are narrow. According to the established standards, there is no presence of anomalous phases in the synthesized materials. The characteristic peaks of the CeO2 crystal phase are clearly observed at angles of 2θ = 28.6°, 33.1°, 47.5°, 56.2°, 59.1°, 69.2°, 76.8°, and 79.0°. This research result is highly consistent with other previously published works [125,126].

3.1.1.4. UV-Vis and FT-IR spectra of CeO_2 nanomaterials

The synthesized material was also evaluated for its ability to absorb UV radiation using UV/Vis-DR spectroscopy, which was applied to powdered samples. The UV-Vis spectral results of the nano CeO_2 material in this study are shown in **Figure 3.5**. It was observed that the peak absorption of the CeO_2 nano material in this study is at 348 nm. This is a wavelength inside the UV

range, consistent with the previous prediction. This result is also quite close to the results obtained in several previous publications using various synthesis methods (**Table 3.3**). This demonstrates that the combustion method of burning PVA gel is suitable for synthesizing CeO_2 nano materials.

3.1.2. Characteristics of the structure and morphology of nano Fe_2O_3

3.1.2.1. Thermalgravimetric analysis of the gel (Fe^{3+}+PVA)

3.1.2.2. SEM images nano Fe_2O_3

3.1.2.3. XRD pattern of nano Fe_2O_3 with calcination temperature of 400 °C

3.1.3. Characteristics of the structure and morphology of nano SiO_2

3.1.3.1. Thermalgravimetric analysis of the gel (Si^{4+}+PVA)

3.1.3.2. TEM images nano SiO_2

3.1.3.3. FT-IR spectra of SiO_2 with calcination temperature of 550 °

3.1.3.4. XRD pattern of nano SiO_2 with calcination temperature of 550 °C

3.2. Characteristics of the structure and morphology of CeO_2-SiO_2 nanocomposite

3.2.1. XRD pattern of CeO_2 -SiO_2 nanocomposite

The XRD pattern of the CS550 sample exhibits a broad characteristic peak at an angle of around 22.0°, indicating the initial development of SiO2 cristobalite crystalline phase. As the temperature increases, the characteristic peaks become sharper and higher in intensity, indicating a transition from the amorphous phase to the crystalline phase [136]. In general, higher heating temperatures result in higher crystallization degrees because when crystals have enough energy, they may self-orient to achieve the highest atomic density and certainly benefit from surface energy [137]. In this study, additional energy is supplied by the combustion of gel components and the decomposition process of PVA, nitrate, and ethyl group. Based on our previous research and those of other authors, PVA begins to degrade at temperatures ranging from 130 to 450 °C [138,139]. However, in order to completely eliminate excess carbon, the required temperature for combustion should reach around 600 °C [140,141]. The results of this study indicate that the highest crystallization efficiency was achieved at 650 °C (**Figure 3.14**). If we continue to increase the temperature, the crystal structure will be disrupted, resulting in the formation of different phases. It can be observed that characteristic peaks assigned to the cristobalite phase of SiO_2 are seen at angles of 21.9, 28.4, and 36.1° (JCPDS number 01-077-8627), corresponding to the crystal planes (101), (102), and (200) [135]. However, at temperatures beyond 750 °C, the peak intensity at 21.9° decreases along with the appearance of two smaller peaks at angles 2θ ~ 20.8° and 23.3° (Figure 3.15). This demonstrates the transformation of the cristobalite SiO_2 phase into the tridymite SiO_2 phase [135]. Similar observations have also been reported in other documents [136].

In addition to the characteristic peaks of SiO_2, the XRD results also indicate the presence of peaks assigned to the cerianite phase of CeO_2. The characteristic peaks of cerianite phase are observed at the respective 2θ angles of 28.7°, 33.2°, 47.4°, and 56.1°, corresponding to the crystal planes (111),

(200), (220), and (311) [125,126]. These vertices are assigned to the face-centered cubic crystal structure of cerianite with Fm-3m space group (JCPDS number 00-054-0593) [142]. The absence of any presence of a peak indicating the formation of an external structure in the CS-NC composite is also clearly demonstrated in Figure 3.14. The results have been reconfirmed by FT-IR and SEM imaging.

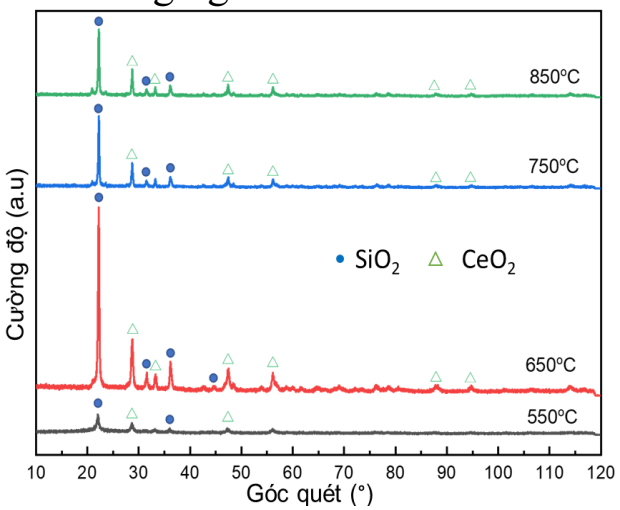

Figure 3.3. XRD pattern of CS-NC at different calcination temperature

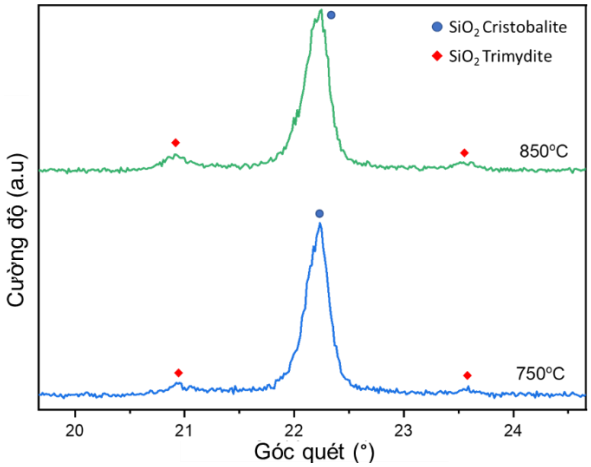

Figure 3.4. XRD pattern of CS-NC at 750 °C và 850 °C (**CS750, CS850**) with 2θ from 20° to 25°

3.2.2. FT-IR spectra, SEM image and EDX of CeO_2 -SiO_2 nanocomposite

CS650 is selected due to its superior crystallization performance achieved at a melting temperature of 650 °C. At this melting temperature, there are no carbon residues, and the CeO_2 and SiO_2 crystal phases may be clearly seen. The FT-IR spectrum exhibits a peak at around 1071 cm-1 and a shoulder at around 1200 cm^{-1}, corresponding to the asymmetric stretching vibration of Si-O-Si [91]. Almeida and Pantano assert that peaks and shoulders originate from the horizontal and vertical oscillations of Si-O-Si [143]. The FT-IR results also indicate a vibration at around 790 cm^{-1}, attributed to the stretching vibration of Si-O-Si [22]. The previous literature often reported that the oscillation regions at 3500-3200 cm^{-1} and 1600-1500 cm^{-1} correspond to the stretching and bending vibrations of water molecules adsorbed on the surface [144,145]. However, these oscillations were not seen in our study, indicating the complete elimination of water molecules adsorbed on the surface of the nanocomposite material. Theo Ho and colleagues predict that the stretching vibrations of Ce-O will have an absorption region from 400 to 450 cm^{-1} and cannot be distinguished from the stretching modes of silica [146]. However, **Figure 3.16** demonstrates that the asymmetric stretching vibration region of Si-O-Si in CeO_2-SiO_2 at 1071 cm^{-1} has shifted. This can occur due to the influence of CeO_2 on the structure of SiO_2 or the bonding of positively charged xeri ions with the highly electronegative oxygen of silica nano particles [147,148].

The results indicate that the SEM image of the nanocomposite, when annealed at 650 °C, exhibits high uniformity and a high degree of porosity. Afterwards, the **CS650** material is used to disperse into the PU substrate in order to enhance the UV resistance capability of the coating layer.

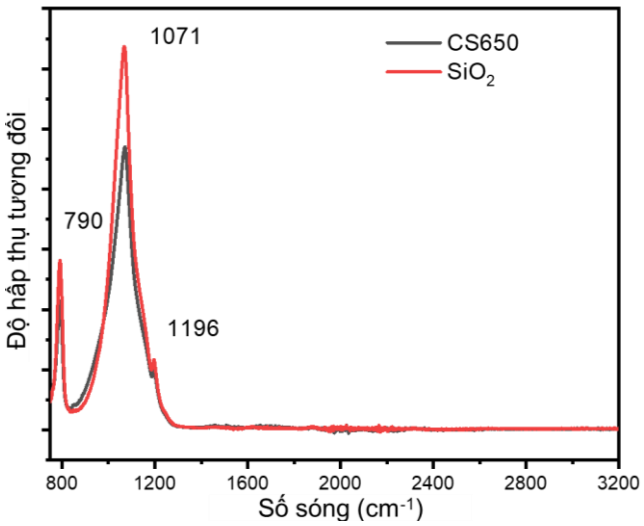

Figure 3.5. FT-IR spectrum of the CS650

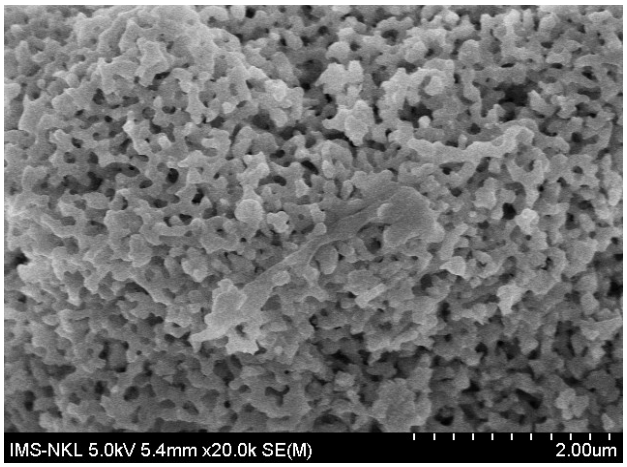

Figure 3.6. SEM image of CS650

3.3. Characteristics of the structure and morphology of CeO_2-Fe_2O_3@SiO_2 nanocomposite

3.3.1. The crystal structure of CeO_2-Fe_2O_3@SiO_2 nanocomposite

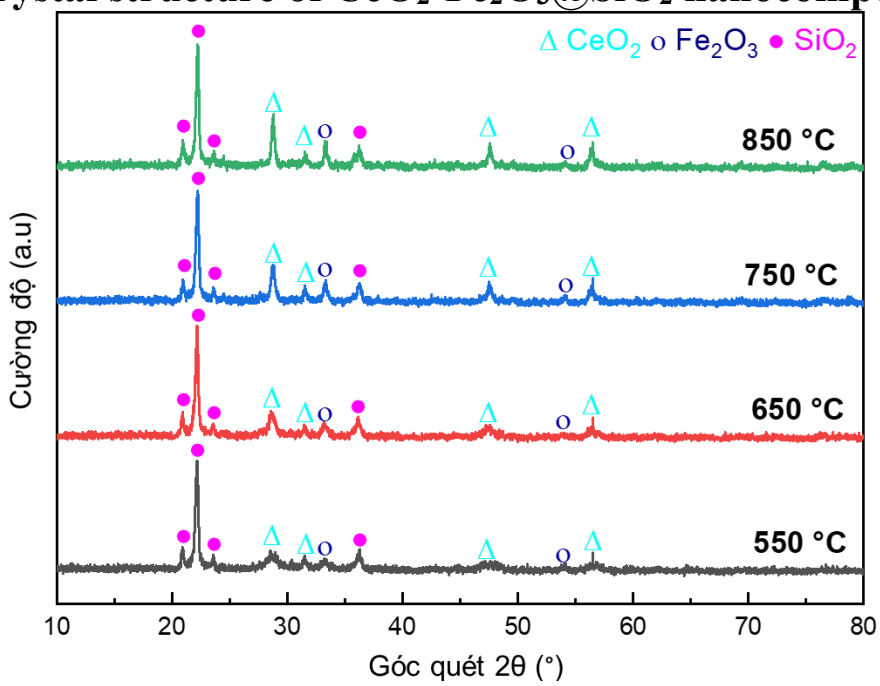

Figure 3.7. XRD pattern of CFS-NC at different calcination temperature

It can be observed that the characteristic peaks of tridymite phase of SiO2 are seen at angles of 20.9°, 22.1°, 23.6°, and 36.2° [135]. The intensity of these peaks remains relatively constant for all materials, indicating a rather good crystallinity of the SiO_2 component. In addition to SiO_2, the XRD results also indicate the presence of peaks assigned to the cerianite phase of CeO_2 and the hematite phase of Fe_2O_3. The characteristic peaks of cerianite CeO_2 are observed at 28.7°, 31.5°, 47.6°, and 56.4°, while the peaks assigned to hematite Fe_2O_3 are seen at 33.3° and 54.1° [133]. Ultimately, the CeO_2 and Fe_2O_3 components of the nano particles were heated at a higher temperature, resulting in a higher degree of crystallization due to their XRD peaks having a greater intensity. Due to this reason, the material is synthesized at a melting temperature of 550 °C (CFS550) in order to save fuel. For the purpose of

enhancing the PU coating on CFS-NC materials, the CFS550 material will be utilized in the experiments.

3.3.2. FT-IR spectrum of CeO_2-Fe_2O_3@SiO_2 nanocomposite

The functional groups and surface linkages of nano materials are investigated using the FT-IR spectroscopy method (**Figure 3.20**). The FT-IR spectrum of these compounds exhibits a peak at around 1068 cm^{-1} and a shoulder at around 1200 cm^{-1}, corresponding to the asymmetric stretching vibration of the O-Si-O bond [91]. Almeida and Pantano assert that the peaks and valleys originate from the transverse and longitudinal components of this oscillation, respectively [143]. The FT-IR results also indicate a peak at around 787 cm^{-1}, which is assigned to the bending vibration of the O-Si-O bond [149]. It is worth noting that all peaks of the material annealed at 550 °C are wider compared to the material annealed at 650-850 °C, indicating a higher degree of bond disorder and lower crystallinity. Lastly, no peaks were observed in the range of 3300 to 3700 cm^{-1}, indicating the complete removal of adsorbed water molecules from the surface of these nano particles.

3.3.3. TEM image và EDX of CeO_2-Fe_2O_3@SiO_2 nanocomposite

The morphology is investigated using TEM analysis (**Figure 3.21**). The image demonstrates the rather uniform nature of the nano-sized material, as confirmed by the measurement of particle size distribution (**Figure 3.22**).

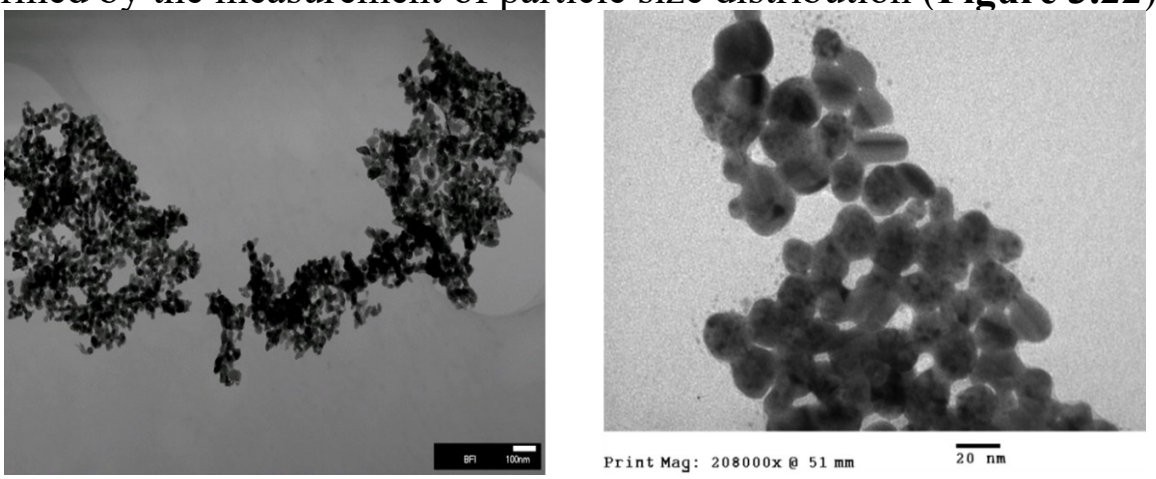

Figure 3.8. TEM images of CFS-NC

3.4. The impact of nanomaterials on the mechanical properties of polyurethane coatings

3.4.1. The dispersibility of CeO_2 nanoparticles, Fe_2O_3 nanoparticles, and SiO_2 nanoparticles in PU

3.4.2. The dispersibility of nanocomposites in PU

Figure 3.25a displays the SEM image of the original PU coating before dispersing the CS-NC material, whereas **Figures 3.25(b)**, **(c)**, **(d)**, and **(e)** correspond to synthetic materials with CS-NC content of 0.25%, 0.5%, 1.0%, and 2.0% respectively. The finer structure of the coating layers significantly reduces the visibility of small cracks on the surface of any nanocomposite content at the given resolution. In reality, due to weak intersegmental bonding (**Figure 1.2**) in the PU, small cracks begin to occur at points on the surface of the coating layer. These cracks continue to expand under the influence of

weather pressure, oxidative agents (such as oxygen, UV rays, temperature, water, salt) [118]. The propagation of cracks into the deep layers of the coating results in significant fracture or delamination of the coating (**Figure 3.25a**). When the coating contains CS-NC, the strong surface interaction between CS-NC and PU can enhance durability. The interaction occurs because to the high surface polarity of CS-NC, facilitating the easy formation of bonding centers with functional groups in PU. However, the excessive addition of CS-NC will cause it to self-aggregate and hinder dispersion, resulting in reduced durability [119]. Chang and colleagues describe that the high concentration of inorganic micro particles can enhance the degradation of polymer structures [151]. However, this research result demonstrates that the mechanical properties of the coating are maintained even with a CS-NC content of up to 2.0% by weight. The results regarding the durability of the coating are also included in Table 3.5. Furthermore, a high level of dispersion will enhance homogeneity (at low CS-NC concentrations). In nanocomposites with high concentrations (>1.0 mass), the random appearance of large particles on the surface of the PU coating layer (white dots in **Figure 3.25d**, **3.25e**) is due to the strong self-aggregation of small-sized nano particles.

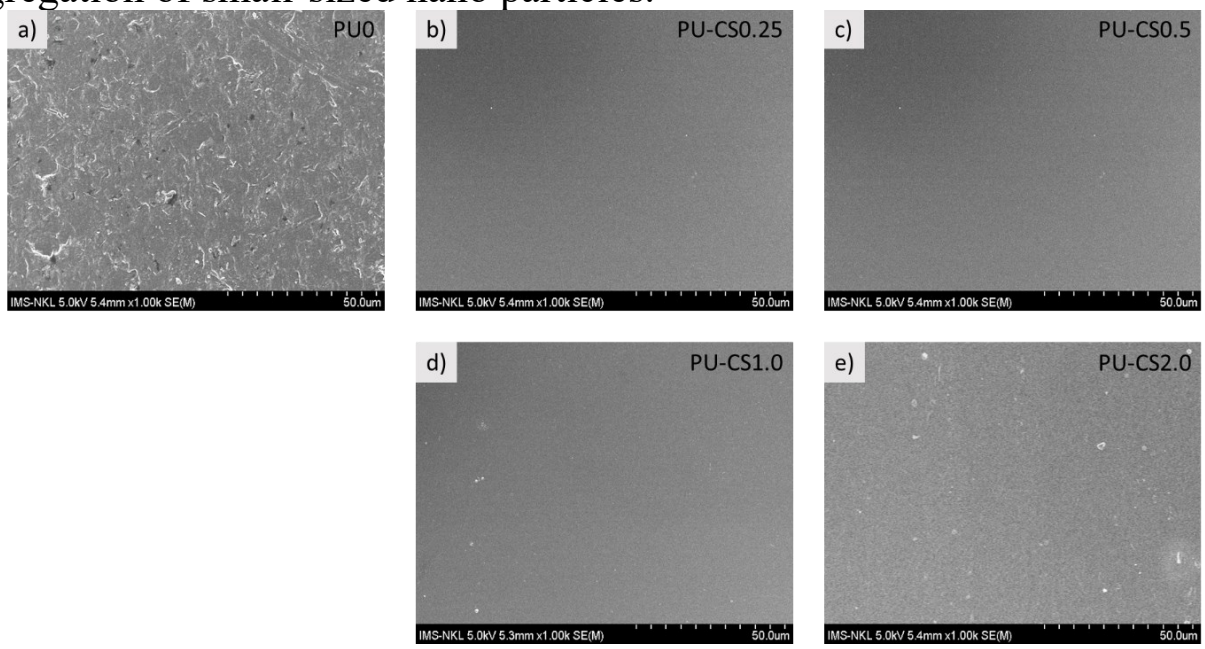

Figure 3.26. SEM image of (a) standard PU và (b-e) PU with different content of CS-NC.

3.5. The impact of CeO_2 nanomaterials on the UV resistance ability of PU coating

The results in **Figure 3.27** demonstrate that the presence of CeO_2 at a concentration of 0.5% (**PU-Ce0.5**) leads to a negligible decrease in gloss deviation over 700 hours. The value of GU decreased from 93 at 100h to just 62 at 700h in the morning. Meanwhile, PU-Ce0.5 only decreases by 5 GU after 700 hours of exposure to light (from 95 GU to 90 GU). Based on these results, we can conclude that the coating exhibited a relatively good resistance to UV radiation compared to the material without CeO_2 (**PU0**).

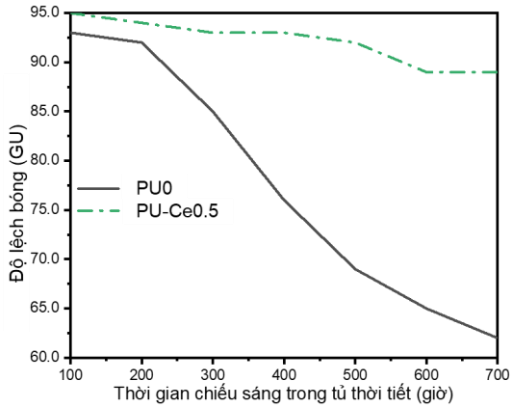

Figure 3.27. Gloss of PU coating under UV irradiation during 700h

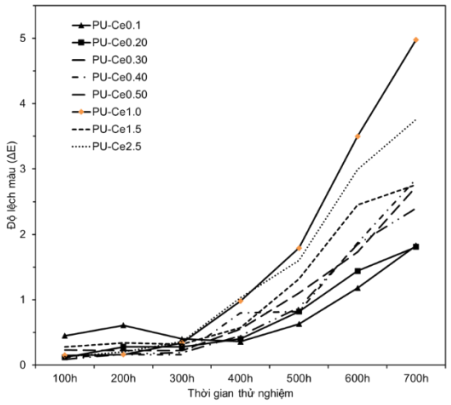

Figure 3.29. Color difference of PU coating with different content of CeO_2 nanoparticles during 700h

Color deviation is also one of the values that may be used to assess the deterioration of a coating. The variation in color deviation of the PU coating with different concentrations of CeO_2 nanoparticles is presented in **Figure 3.27**. During the first 350 hours, with varying concentrations, the coating still exhibited consistent relative color deviation. After 400 hours, the difference in concentration shows a more pronounced trend. Overall, coatings with lower concentrations of CeO_2 nanoparticles exhibit lower color deviation with time. This may be attributed to the inherent yellow color of CeO_2 nanoparticles, which, at higher concentrations, result in a more pronounced difference in color.

3.6. The impact of CeO_2-SiO_2 nanocomposites on the UV resistance ability of PU coating

3.6.1. UV-Vis spectrum of PU-CS

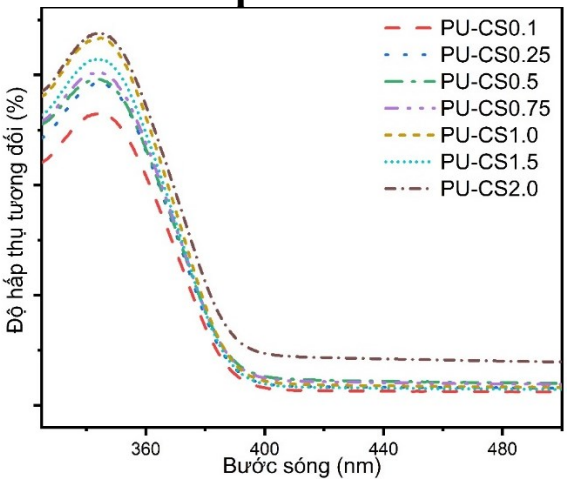

Figure 3.30. UV- Vis spectrum of PU-CS.

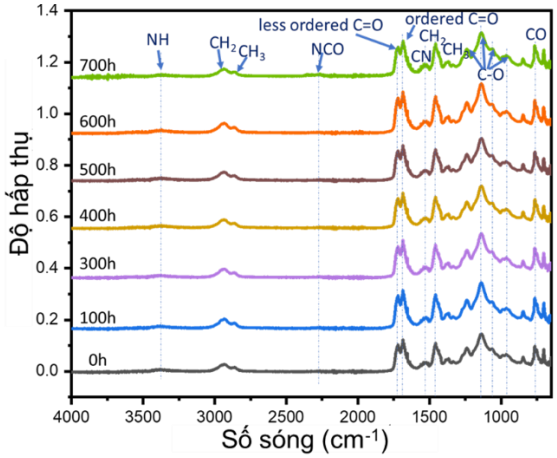

Figure 3.31. FT-IR spectrum of **PU-CS1.0** during 700h under UV irradiation

The peak absorption occurs at 344 nm and at around 400 nm. This absorption band belongs to UVA radiation [152]. At relatively low CS-NC concentrations (<2%), the absorption range shifts towards the UVA region, possibly due to the characteristics of CeO_2 particles [152]. The UV absorption capacity of the material gradually increases with the increase of CS-NC content from 0.1% by weight to 1% by weight, except for **PU-CS1.0** and **PU-CS1.5**. As we discussed in the last section, a higher concentration of material

might lead to the aggregation of nano materials. With a CS-NC concentration over 1% by weight, it is possible to observe some large particles (Figure 3.25c, 3.25d). The presence of large particles can affect the absorption capacity of the coating layer. The result is that the absorption capacity may not increase linearly with the CS-NC concentration. The incorporation of CS-NC into PU coatings is expected to have applications as an outdoor protective layer.

3.6.2. FT-IR spectrum of PU-CS during 700h under UV irradiation

In the image, the observation of the wavelength associated with the nanocomposite is not possible because to the overlapping of high-intensity oscillations and the position of the PU background. An analysis revealed the presence of a little variation within the 2250-2300 cm^{-1} range, suggesting the residual isocyanate group (-NCO) of the isocyanate (curing agent) in the PU coating at the start (0h) [153]. It indicates that the presence of nano particles in the solvent delays the solidification process or indicates that the reaction is not yet complete. In general, by monitoring the FT-IR spectral changes, different trends in the degradation process of the original PU coating structure and the coating with dispersed nano materials may be identified. The oscillations are assigned to different functional groups of the C=O bond around the region of 1700 cm-1 (including symmetric or asymmetric vibrations). In general, the higher the degree of the C=O bond, the greater the wavelength. Therefore, the vibrations at 1685 cm^{-1}, 1681 cm^{-1}, and 1676 cm^{-1} correspond to the NH–(C=O)–NH bond in polyurea, whereas the wavelengths at 1724 cm^{-1} and 1719 cm^{-1} correspond to the stretching vibrations of the C=O bond in PU. This has also been demonstrated in previous studies on C=O bonding. Vibrations in the range of 1635 to 1703 cm^{-1} indicate the presence of ordered C=O structures, whereas vibrations in the range of 1703 to 1735 cm^{-1} indicate the presence of less ordered C=O structures [154,155]. Under prolonged exposure to UV light (700h), the coating appears to undergo some changes in molecular structure, as indicated by an increase in the intensity of oscillation at 1724 cm^{-1} and 1719 cm^{-1}, along with an increase in the stretching vibration at wavelengths 1685 cm^{-1}, 1681 cm^{-1}, and 1676 cm^{-1}. This can be explained by the circuit splitting of the PU coating layer leading to the reconnection of polyurea molecules [156]. The possibility of different occurrences on the surface of the coating layer and the formation of new carbonyl groups, particularly the formation of polyurea, may be observed when certain groups undergo oxidation [157].

The FT-IR spectrum exhibits a characteristic vibration in the range of 3100-3500 cm^{-1}, which is specific to the stretching vibrations of NH groups bonded to hydrogen atoms [158,159]. The intensity of this oscillation decreases as the exposure time to UV light increases, indicating the loss of urethane structure [160]. What is interesting is that this research result demonstrates a slight variation in the oscillation region (Figure 3.32A). The N-H stretching extends from 3370 cm^{-1} onwards, indicating overlapping vibrations of different N-H bonds [156]. Another interesting characteristic is the presence of an oscillation around 2862 cm^{-1}, believed to be caused by the

stretching of the C–H_2 bond. This association appeared to increase after 700 hours of UV exposure. Additionally, other oscillations were observed at 2862 cm^{-1} (stretching -CH_2-H) and 1454 cm^{-1} (bending -CH). The oscillations at 1238 cm^{-1}, 1137 cm^{-1}, 1064 cm^{-1}, 962 cm^{-1}, and 764 cm^{-1} (characteristic region of polymer [158]) are associated with the CO bond and show a little increase (**Figure 3.32B**). To explain these changes, we must start with the adsorption of oxygen molecules in the air on the surface of the PU coating layer [161]. Afterwards, under UV radiation, the formation of corresponding organic radicals (R-NH●, R CH_2-CH_2●, R-CH-OO●) leads to the cleavage of CN and CO bonds. This process releases gases mostly composed of CO_2 and CO, with small amounts of H_2, CH_2O, and HCN, as shown in **Figure 3.33** [162].

In addition, water-loving groups such as aldehydes, carbamates, carboxylic acids, amine esters, and peresters are formed [156]. Gradually, it leads to the formation of defects on the surface of polyurethane, including voids, cracks, and blisters. The cleavage of polymer molecule chains occurs on the surface of the polymer, resulting in the formation of polymer radicals. These intermediate products can join with the main chain of neighboring molecules to form a branched chain with a higher molecular weight (cross-linking). Due to this factor, it leads to high stress and excessive brittleness caused by the formation of these cross-linking molecules, which appears to be the main cause of microcracks and fractures [163]. Overall, it leads to changes in material properties, such as increased surface roughness and loss of gloss, tensile strength, and color.

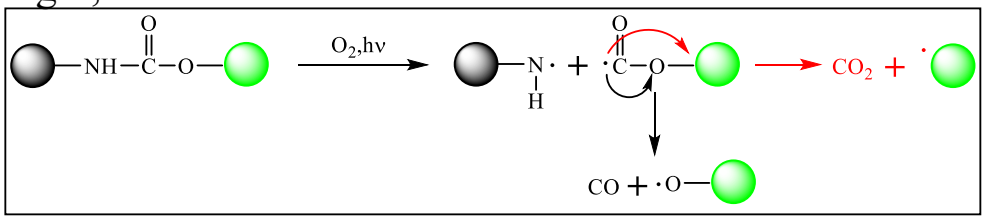

Figure 3.33. The urethane bond degradation mechanism of the PU coating layer results in the formation of CO and CO_2 gases.

3.6.3. Gloss and color deviation of PU-CS during 700h under UV irradiation.

Figure 3.35 illustrates the variations in color and glossiness of the PU coating supplemented with different concentrations of CS-NC. The difference in color in the PU coating when exposed to prolonged UV rays is seen in **Figure 3.35a**. The CeO_2 nanoparticles exhibit a pale yellow color [18], which is clearly visible in the image. The color deviation tends to increase as the nanocomposite content increases (**Figure 3.35a**, Supplementary Appendix Table S1). However, the mass ratio of CS-NC ranges from 0.1% to 2.0%. Therefore, the difference in color is negligible. Generally, the **PU0** exhibits the highest degree of color variation (Appendix Table S1). When comparing, the discrepancy ratio between **PU-CS0.1** and **PU-CS2.0** increases gradually and may be observed as a noticeable difference. Under prolonged exposure to UV radiation, the color of the PU coating gradually shifts, mostly due to the gradual degradation of the coating on the surface [15]. **Figure 3.35a**

demonstrates that the PU coating in this study exhibits highly effective UV protection, particularly in resisting color fading during weathering tests. For example, Jalili and Moradian reported a ΔE value of 2-4.8 after 200 hours for the PU coating with added SiO_2 nanoparticles in the QUV weathering cabinet, whereas Saadat-Monfared and colleagues reported a ΔE value of 1-1.2 for the PU coating with added CeO_2 nanoparticles after 700 hours of exposure to weathering [48]. This difference is a strong indicator of the effectiveness of CS-NC as a UV-absorbing agent in PU coatings.

The loss of glossiness in the polyurethane film is mostly due to the increase in roughness caused by the formation of surface defects [14]. Once again, the white PU coating (**PU0**) exhibits the fastest rate of decay, followed by **PU-CS2.0** (**Figure 3.35b**). When comparing, **PU-CS0.1** and **PU-CS1.5** demonstrate an equal level of gloss loss, followed by **PU-CS0.25** to **PU-CS1.0**. From 400 to 700 hours, the deviation of the **PU-CS1.5** ball from the **PU-CS0.1** ball increases significantly, possibly due to the formation of surface damage. The glossiness of the PU coating is maintained at a level of 93 GU for **PU0**, **PU-CS0.1**, and **PU-CS0.25** (Appendix Table S2), increases to 95 GU for **PU-CS0.5** before gradually decreasing to 89 GU for **PU-CS2.0** (**Figure 3.35b**, Appendix Table S2). The phenomenon of decreasing glossiness is likely to persist due to the influence of UV rays. However, this research shows that the presence of CS-NC in the PU coating significantly reduces surface damage to PU material by just 0.25-1% of CS-NC material.

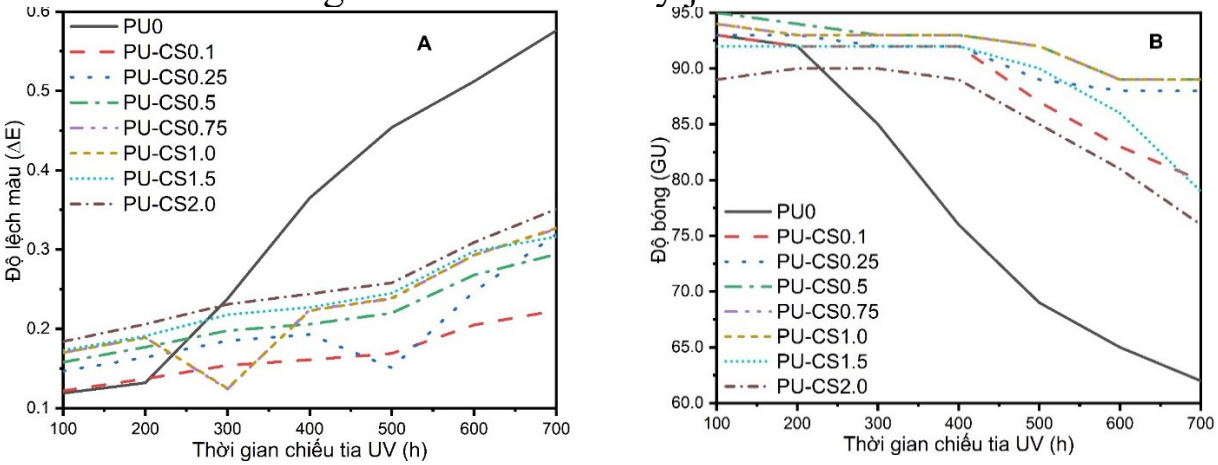

Figure 3.35. The changes in a) color deviation and b) gloss of the PU with different content of CS-NC under UV irradiation.

3.7. The impact of CeO_2-Fe_2O_3@SiO_2 nanocomposites on the UV resistance ability of PU coating

3.7.1. The impact of CFS material on the bonding of PU coating

3.7.2. FT-IR spectrum of PU-CFS during 700h under UV irradiation

The **PU0** to **PU-CFS1.0** films have been selected for long-term UV exposure testing. The common degradation pathway of PU film by UV radiation is illustrated in Figure 3.39 [161]. **Figure 3.39** illustrates that the surface of the PU membrane absorbs oxygen molecules from the air. It induces the formation of corresponding organic radicals (R-NH·, R CH_2-CH_2·), leading to the cleavage of CN and CO bonds. This process releases gases mostly

composed of CO_2 and CO, with small amounts of H_2, CH_2O, and HCN. At that time, water-loving groups such as aldehydes, carbamates, carboxylic acids, amine esters, and peresters were formed [156]. The formation of hydrophilic groups promotes the adsorption of moisture. During exposure to the environment, temperature and humidity fluctuations cause the PU surface to expand and contract. Gradually, it leads to the formation of defects on the surface of PU, including voids, cracks, and blisters. Overall, it leads to changes in the properties of the material, such as increased surface roughness and loss of gloss, decreased tensile strength and color. Generally speaking, double-bonded conjugated membranes are more susceptible to degradation compared to other saturated polymer such as PE and PP.

The presence of nano particles in the polymer matrix can inhibit the degradation of the polymer structure by the mechanism explained above, to a certain extent. Specifically, they can absorb, reflect, and scatter UV rays. Therefore, it reduces the amount of UV rays that cause polymer degradation. Furthermore, they can entrap the roots formed during the polymer degradation process, therefore slowing down the degradation process. This protection depends on the composition, dimensions, and thickness of the materials layers. In general, smaller particle sizes allow for better absorption of ultraviolet rays, whereas appropriate particle sizes provide optimal scattering of ultraviolet light [45,165]. Furthermore, it is crucial for the nanoparticles to have an appropriate bandgap width in order to effectively absorb UV rays.

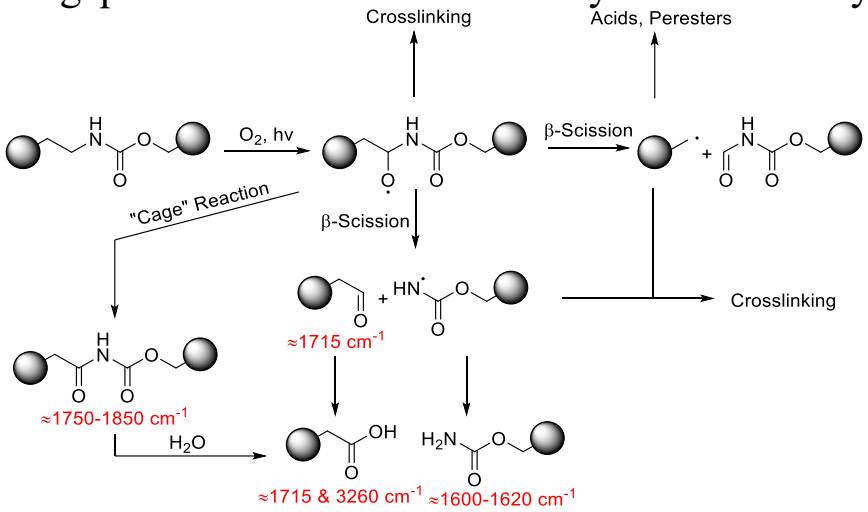

Figure 3.39. Certain pathways of degradation can occur during prolonged exposure to ultraviolet radiation.

The **PU-CFS** coating is also evaluated for changes in bonding using the FT-IR method. However, in this study, we made some minor adjustments compared to the research method conducted by Cascaval et al. in the previous chapter to monitor the FT-IR spectrum changes of the selected **PU0** and **PU-CFS1.0** coating after exposure to UV radiation (**Figure 3.40**) [160]. The result is obtained by extracting the difference in FT-IR intensity at two different time points. For example, Δ(100) represents the intensity difference between 100 and 0 hours, while Δ(200) represents the intensity difference between 200 and 100 hours. The vertices with negative values represent the loss of

corresponding functional groups, whereas the vertices with positive values represent the formation of new functional groups.

It can be observed that the formation and loss of -OH and -NH groups (in the broad range of 3200-3500 cm^{-1}), C=O bonds (1700-1750 cm^{-1}), saturated C-C bonds (1300-1400 cm^{-1}), and C-O bonds (1000-1250 cm^{-1}) have been detected. Within the range of 3300-3700 cm^{-1}, significant changes attributed to the -OH and -NH groups have been observed for PU0, whereas PU-CFS1.0 shows no significant changes. Overall, monitoring the spectral changes in FT-IR reveals different trends in the degradation process of both white PU film and film containing nano materials.

The dispersion of nano particles into the PU matrix can initiate the process of restructuring the hydro network and polymer bonding. This modification contributes to enhancing the other properties of the membrane. In Feng et al.'s study, the abrasion resistance of the PU coating increased tenfold after the addition of 2.0 wt% SiO_2 [166]. In Liu et al.'s study, the contact angle with water of PU increased from below 120 to 151° by adding 20% of SiO_2 by weight [167].

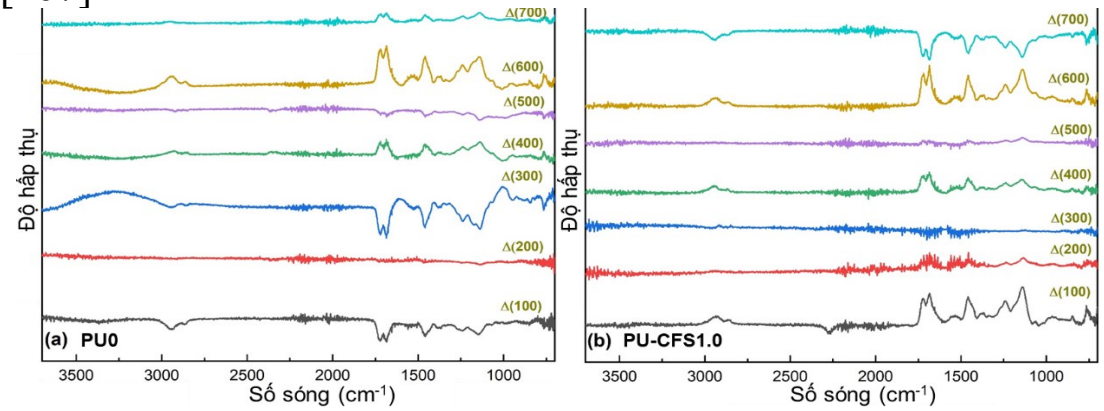

Figure 3.40. The differences observed in the FT-IR spectra of the white **PU0** film and the **PU-CFS1.0** film under UV exposure in the accelerated weathering testing.

3.7.3. Color deviation and gloss of PU-CFS during 700h UV irradiation.

The wetting ability of polyurethane film depends on its water affinity, surface roughness, and surface free energy of the material. It may be evaluated by measuring the contact angle with water (WCA). WCA dưới 90° được xếp vào danh mục ưa nước, trong khi WCA trên 90° được xem là kỵ nước. On the other hand, a contact angle more than 150° is considered superhydrophobic, while a contact angle less than 5° is considered superhydrophilic. In Zhang et al.'s study, it was shown that humidity increases with increasing roughness on hydrophobic surfaces and decreases with increasing roughness on hydrophilic surfaces [168]. Regarding this issue, our materials have a slight hydrophilic property, measuring 89° for **PU0** to **PU-CFS1.5** and 86° for **PU-CFS2.0**. The higher value of **PU-CFS2.0** may be attributed to an increase in material roughness due to the concentration of nano particles exceeding the limit.

As shown in **Figure 3.42a**, the WCA of all PU membranes decreases due to the degradation of the polymer structure during UV irradiation in the weathering cabinet. During this process, new C=O bonds are formed and result

in surface damage. The formation of hydrophilic C=O bonds increases the hydrophilicity of the surface, while surface damage increases roughness or reduces glossiness. The overall reduction rate of WCA decreases in the following order: **PU0** > **PU-CFS1.5**, **PU-CFS2.0** > **PU CFS1.0**, and finally **PU CFS0.1**. The appropriate amount of nano particles (0.1-1.0 wt%) inside the PU matrix aids in the reflection, dispersion, and absorption of UV rays. Comparatively, the excessive combination of nano particles (at 1.5 and 2.0% by weight) demonstrates the adverse effects caused by the agglomeration of nano particles and the ability to reorganize the structure as well as fracture the hydrogel network.

The loss of glossiness in the PU film is mostly caused by an increase in surface roughness due to the formation of surface defects. Once again, **PU0** exhibited the fastest decrease in brightness, followed by **PU-CFS2.0** (**Figure 3.42b**). When comparing, **PU-CFS0.1** and **PU-CFS1.5** exhibit similar levels of gloss loss, followed by **PU-CFS0.25** to **PU-CFS1.0**. From 400 to 700 hours, the rate of gloss loss of **PU-CFS0.25** to **PU-CFS1.0** significantly increases, possibly due to the formation of surface damages.

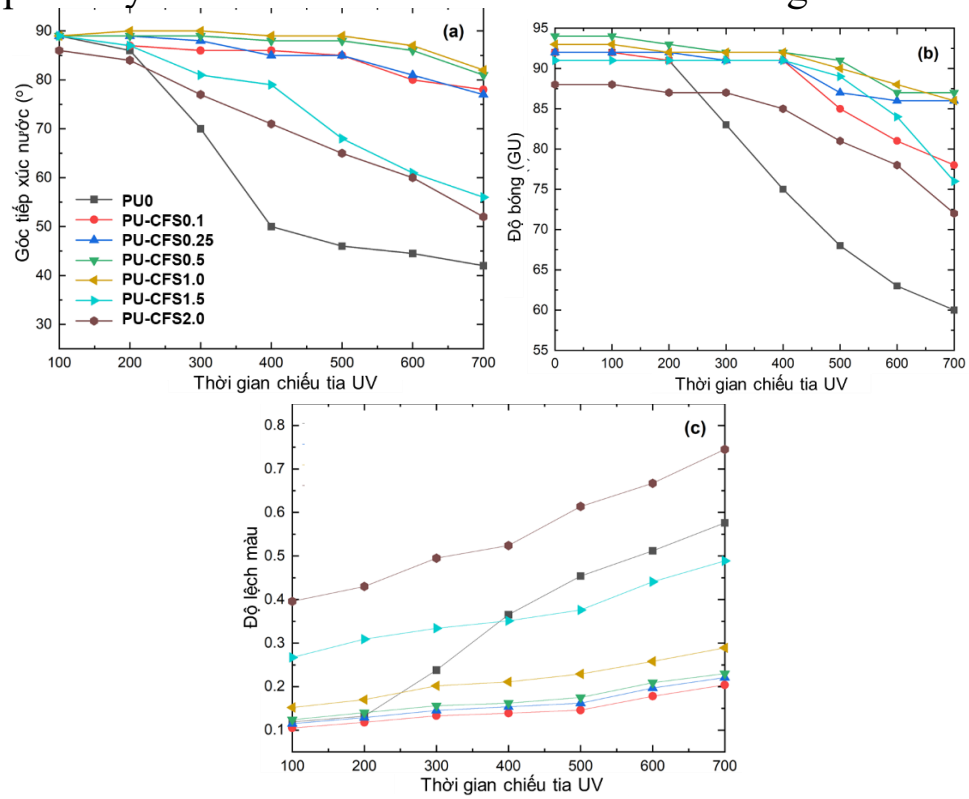

Figure 3.42. The addition of CFS-NC to the PU film during UV testing in the weathering chamber results in changes in the contact angle with water (a), glossiness (b), and color (c).

Under prolonged exposure to UV radiation, the color of the polymer gradually changes. The difference in color in the PU film when exposed to prolonged UV rays is seen in **Figure 3.42c**. The **PU0** has the highest color deviation rate. When comparing, the discrepancy rate of **PU-CFS0.1** to **PU-CFS2.0** is lower and almost equivalent to each other. Overall, there is no clear relationship between WCA, changes in glossiness and color deviation, as well as differences in FT-IR spectra, as shown in **Figure 3.42**.

The CeO_2-Fe_2O_3@SiO_2 nanocomposite material has been successfully synthesized using a multi-step sol-gel combustion method, with an average size of around 20 nm. The characteristic properties of materials are also investigated using modern methods. Generally, the optimal concentration of CeO_2-Fe_2O_3@SiO_2 nano particles in the PU coating ranges from 0.1 to 1.0% by weight. It can be observed that at low concentrations, the UV resistance of the **PU-CFS** coating is more effective than that of **PU-CS** and **PU-Ce**. This can be explained by the presence of an additional component, Fe_2O_3. The interconversion between the oxidized states Fe_2O_3/Fe_3O_4 [97] in combination with the vacancies on SiO_2 leads to the rapid quenching of the generated electron-hole pairs. The photogenerated process of CeO_2 under UV irradiation does not generate free radicals, but instead rapidly converts into thermal energy, hence providing more effective protection for the PU coating. Furthermore, the incorporation of **CFS-NC** particles containing Fe_2O_3 into the PU membrane structure exhibits some superior properties, such as thermal stability. The results of the study on the thermal durability of the PU coating are presented in the next section.

3.8. The impact of CeO_2-based nanocomposite materials on the thermal stability of PU coatings

The thermal stability of the PU film increases with the increase in the number of urethane groups and the formation of urethane-urethane crystalline domains [169]. The thermal degradation mechanism of polyurethane membranes is discussed in detail in the previous document [170]. Decomposition often starts at the weakest bonding sites of conventional materials, such as on the surface or at the interfacial junctions between material layers. In previous studies, this process has been considered to begin when a loss of around 5.0% in weight is seen [171,172]. In this study, the degradation process of **PU0** membrane is characterized by three stages occurring between 240 and 580 °C [173]. The first stage is observed at temperatures ranging from 240 to 370 °C, with a weight loss of 44.1%. This loss corresponds to the rupture of the urethane region [174,175]. The second phase occurs between 370 and 470 °C, resulting in a 24.2% reduction in weight due to the decomposition of the polyol region [176]. The last stage occurs between 470 and 580 °C, during which the material undergoes decomposition, resulting in the formation of various residues, such as primary amines, secondary amines, and ethers. This residue serves as a thermal barrier, preventing further material degradation. The residue weight of **PU0** film is 18.1% by weight.

Previous studies have demonstrated that metal oxide nanoparticles have the ability to enhance the thermal resistance properties of PU coatings [177]. In this study, **PU-CFS1.0** exhibits a higher thermal resistance of 320 °C compared to **PU0**. One plausible explanation for this enhancement might be attributed to the reduced flexibility of the urethane domains inside the polymer matrix [178]. At temperatures ranging from 320 to 380 °C, **PU-CFS1.0** experiences a weight reduction of 7.5%. Afterwards, from 380 to 450 °C, **PU-**

CFS1.0 exhibits rapid and significant degradation (decreasing 69.1% in weight), followed by minor degradation from 450 to 540 °C (decreasing 13.5% in weight). Both decomposition processes (380 to 540 °C) are characterized by the observed heat release properties, as seen on the DSC curve (Figure 3.43c). The heat dissipation property is a result of the thermal effect of the combustion process oxidizing the organic compounds of the PU substrate [179]. Tại nhiệt độ 550 °C, **PU-CFS1.0** có hàm lượng chất rắn còn lại là 9,5% trọng lượng, thấp hơn so với **PU0**. In summary, CFS particles aid in stabilizing the PU membrane at temperatures up to 320 °C. However, at temperatures over 360 °C, the CFS micro particles act as catalysts, accelerating the thermal decomposition process and reducing the percentage of residue mass (thus improving combustion efficiency).

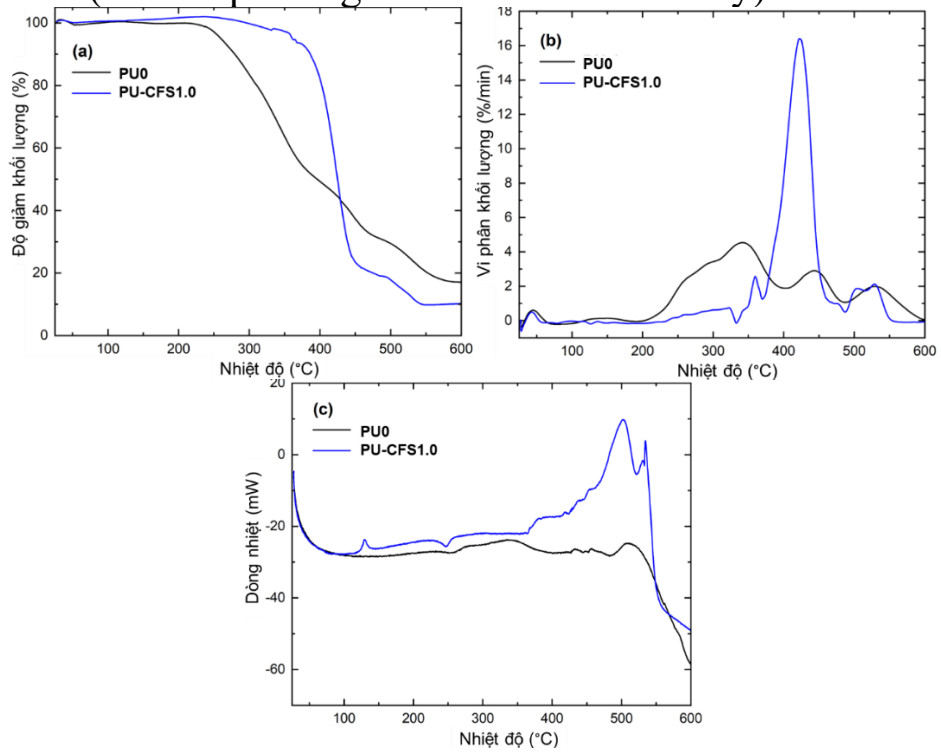

Figure 3.43. The TGA-DSC curves of the **PU0** and the **PU-CFS1.0**.

The results indicate that **CFS-NC** enhances the thermal stability of the material up to a temperature of 320 °C and its resistance to prolonged UV exposure. Meanwhile, CS-NC and nano CeO_2 exhibit thermal stabilities of 259 °C and 256 °C, respectively. This is partly attributed to the reduced flexibility of the urethane domains in the PU matrix, or it may be described as the enhanced surface interaction between the oxide and polymer [94]. This also helps explain why all materials have higher thermal durability than **PU0** (**Table 3.7**). However, **PU-CFS1.0** exhibits the highest thermal stability due to the presence of Fe_2O_3 component in the composite, which increases the ignition temperature of the polymer and therefore enhances the durability of the coating [94].

CONCLUSION

1. Successfully synthesized nano materials SiO_2, nano Fe_2O_3, nano CeO_2, nanocomposite CeO_2-SiO_2, nanocomposite CeO_2-Fe_2O_3@SiO_2 by PVA gel combustion method.

- For CeO_2 nanomaterials: The optimal conditions to synthesize CeO_2 nanomaterials with uniform size (about 30 nm) are pH 4, Ce/PVA molar ratio is 1/3, calcined at 550 °C for 2 hours. Prepared nanoparticles have relatively good UV absorption ability with absorption peak at about 344 nm.

- For CeO_2-SiO_2 nanocomposite materials: The optimal conditions to synthesize CS materials with uniform size (about 30 nm) are pH 4, Ce+Si/PVA molar ratio is 1/3, calcination at 650 °C for 2 hours.

- For CeO_2-Fe_2O_3@SiO_2 nanocomposite material: The optimal conditions to synthesize CFS material with uniform size (about 20 nm) are pH 4, Ce+Fe/PVA molar ratio is 1/3, calcined at 550 °C for 2 hours

2. The dispersion of CeO_2-based nanocomposite materials into PU coating by in situ polymerization and evaluated some physical and mechanical properties and UV resistance of the coating. During 700 hours of testing, the results showed that the coating containing CeO_2-based nanocomposite materials has some superior properties compared to the white PU sample.

- For PU-Ce: The coating has the ability to absorb UV rays with an absorption peak of about 348 nm. The coating also shows good resistance to UV rays, however the agglomeration phenomenon of nano CeO_2 is strong with a density > 1% by weight.

- For PU-CS: CS-NC material is dispersed into the PU matrix better than nano CeO_2. The coating has good UV resistance through color deviation and gloss. **PU0** after 700 hours is distorted by 31 GU, while **PU-CS0.5**, **PU-CS0.75**, and **PU-CS1.0** are only distorted by 6 GU. For color deviation, only 0.5 wt% CS is needed, the color deviation almost does not change significantly after 700 hours of UV irradiation. The optimal ratio of CS-NC material in the coating is from 0.5-1.0% by weight.

- For PU-CFS: CFS-NC material has good dispersion ability similar to CS-NC, the material also shows good ability to absorb UV rays for a long time. Besides, CFS material also enhances the heat resistance of PU coating up to 320 ºC. The optimal ratio of CFS material in PU coating is from 0.1-1.0% by weight.

- The results show that SiO_2 in the nanocomposite enhances the dispersion of the material into the PU matrix while Fe_2O_3 enhances the thermal stability of the coating.

LIST OF PUBLISHED WORKS RELATED TO THE DESSERTATION

1. Porous nonhierarchical CeO_2-SiO_2 nanocomposites for improving the ultraviolet resistance capacity of polyurethane coatings, **2021,** *Materials Research Express*, 8(5), 056405. DOI: 10.1088/2053-1591/abff77
2. Effect of CeO_2-Fe_2O_3 coated SiO_2 nanoparticles on the thermal stability and UV resistance of polyurethane films, **2021**, *Journal of Polymer Research,* 28(4), 1-11. DOI: 10.1007/s10965-021-02487-0
3. Nghiên cứu đặc trưng tính chất của màng sơn polyurethan có chứa vật liệu nano CeO_2, **2021**, *Tạp chí phân tích Hóa, Lý và Sinh học*, 26, 192-195.
4. Mechanical and weather resistance improvement of polyurethane thin films embedded with nanocomposites CeO_2-SiO_2, **2022**, *Vietnam Journal of Catalysis and Adsorption,* 10(1S), 173-179. DOI: 10.51316/jca.2021.117